JOURNAL OF MORPHOLOGY 197:159–181 (1988)

# Muscular Mechanisms of Snake Locomotion: An Electromyographic Study of Lateral Undulation of the Florida Banded Water Snake (*Nerodia fasciata*) and the Yellow Rat Snake (*Elaphe obsoleta*)

BRUCE C. JAYNE
*Department of Developmental and Cell Biology, University of California, Irvine, California 92717*

*ABSTRACT* Electromyography and cinematography were used to determine the activity of epaxial muscles of colubrid snakes during terrestrial and aquatic lateral undulatory locomotion. In both types of lateral undulation, at a given longitudinal position, segments of three muscles (Mm. semispinalis-spinalis, longissimus dorsi, and iliocostalis) usually show synchronous activity. Muscle activity propagates posteriorly and generally is unilateral. With each muscle, large numbers of adjacent segments (30 to 100) show simultaneous activity. Terrestrial and aquatic undulation differ in two major respects. (1) During terrestrial undulation, muscle activity in a particular region begins when that portion of the body has reached maximal convex flexion and ends when it is maximally concave; this phase relation is uniform along the entire snake. During swimming, however, muscle activity passes posteriorly faster than the wave of vertebral flexion, causing the relation of muscle activity to flexion to change along the length of the snake. (2) In the terrestrial mode, the block of active muscle segments remains approximately constant in size as it passes down the snake, whereas during swimming the number of adjacent active muscle segments increases posteriorly. Despite the fact that *Elaphe obsoleta* has nearly twice as many body vertebrate as *Nerodia fasciata* (240 vs. 125), the only difference observed in the swimming of these two species is that a larger number of adjacent muscle segments is simultaneously active in comparable regions of *Elaphe obsoleta* than in *Nerodia fasciata*.

The diversity of snake locomotor modes has been well documented. Lateral undulation, concertina, and sidewinding are the three most commonly used modes in which various patterns of vertebral flexion generate propulsive forces (Gray, '46; Gans, '74; Edwards, '85). In addition to these distinct categories, the existence of certain less common and transitional modes occasionally has been discussed (Gans, '74, '84; Jayne, '86). To date, most work on snake locomotion has dealt with categorizing different locomotor modes and discussing the patterns of force transmission and the interrelationships between the different modes (Mosauer, '32; Gray and Lissmann, '50; Gans, '74, '85).

Concurrent with study of snake locomotion, workers have clarified the anatomy of snake axial muscles believed important for locomotion. The individual segments of these axial muscles usually have a 1 : 1 correspondence with the underlying vertebrae. Each of the individual muscle segments has distinct tendinous and contractile tissue portions. These serially homologous muscle segments collectively form distinct longitudinal columns of muscle, which are apparent upon gross examination (Mosauer, '35; Gasc, '74).

Mosauer's ('35) pioneering work on the axial muscle segments of snakes documented considerable interspecific variation. Individual segments of axial muscles vary in their shape, interconnections with nonhomologous muscle segments, and relative proportion of tendon and contractile tissue. Mosauer attempted to use this variation to

construct a phylogeny of snakes. The more recent, detailed studies of Gasc ('67, '74) illustrated that Mosauer's phylogenetic scheme was greatly oversimplified. A major dichotomy exists between booid and colubroid snakes, and this is clearly manifested in the axial muscles by qualitative differences in shapes and interconnection among muscle segments (Mosauer, '35). However, within colubroids there is much gross qualitative similarity in the shape of the contractile tissue for the largest epaxial muscles such as the Mm. semispinalis-spinalis (SSP-SP), multifidus, longissimus dorsi (LD), and iliocostalis (IC). Furthermore, these major epaxial muscles of colubroids now are known to display a continuum of variation in their interconnections with each other, obscuring Mosauer's distinctions between the colubrid and viperid myological types within the colubroids (Gasc, '74). Substantial quantitative differences also exist in the lengths of the tendinous portions of the various muscles, and this variation is associated with specialization in habitat and habits (Gasc, '74; Jayne, '82). A tendon of a single segment of the M. semispinalis-spinalis may exceed 30 vertebrae in length in certain aboreal species, compared with a length of only six vertebrae in some aquatic species (Jayne, '82).

Despite the parallel study of snake locomotion and musculature, a pattern of muscle activity has not been documented for any of the modes of snake locomotion that rely on vertebral flexion. After measuring coefficients of friction and reactive forces generated by a snake performing terrestrial lateral undulation, Gray and Lissmann ('50) proposed models for the muscular mechanisms of this mode for snakes crawling through a tube with rectangular bends and past various numbers of pegs. For their modeling, Gray and Lissmann assumed the locomotor muscles of snakes spanned only one body segment and that a specific posture was used by snakes gliding past pegs. They concluded that snakes performed this terrestrial mode by using alternating, unilateral, descending muscle contractions. Furthermore, the initiation of muscle contraction was dependent not only on the extent of lateral vertebral flexion, but also on the position of the snake relative to the lateral pivotal points.

Gray ('53) provided another detailed discussion and model for the mechanisms of undulatory locomotion, including the swimming of snakes. In this review, Gray stressed the similarity between terrestrial and aquatic lateral undulation. According to Gray, the primary difference between these two modes is that the waves of lateral flexion move posteriorly with a velocity equal, but opposite to, the velocity of forward progression during terrestrial movement, whereas the wave of bending travels faster than the forward speed of a swimming snake. Hence, the wave of bending remains stationary to the ground for terrestrial undulation but slips backward through the water during swimming. Gray included observational data on the waveform of snakes swimming in media with different viscosities and noted that the external resistive forces encountered by swimming snakes did affect the waveform of the animal. However, Gray did not suggest that this would affect the underlying muscular mechanism of propulsion. In contrast to Gray, Blight ('77) suggested that the balance between the active and passive properties of the body of the swimmer and of the resistance of the medium determines the nature of the swimming mechanism. Blight's discussion particularly emphasized elongate swimmers, whose bodies he predicted to be stiffness-dominated rather than flexibility-dominated. The models of Gray and the concepts of Blight will be examined in more detail later.

Although Gray and Lissmann ('50) modeled aspects of sidewinding and concertina locomotion, they predicted muscular mechanisms only for terrestrial and aquatic lateral undulation. Gray and Lissmann were careful to state most of their assumptions and simplifications when discussing snake locomotion, and their explicit detail provides an excellent theoretical framework that can now be tested experimentally. These models primarily predict the onset and offset of muscle activity rather than amplitude. The key predictions of these models involve the relation of muscle activity to regions of the snake's body that are either concave or convex.

This study used synchronized electromyography and cinematography to determine the onset and offset of muscle activity during terrestrial and aquatic lateral undulation. The activity of the three largest epaxial muscles, the Mm. semispinalis-spinalis, longissimus dorsi, and iliocostalis, was the primary focus of this work. In order to minimize variation in the tendinous interconnections between these three muscles, only colubroid snakes were examined. The colubrids *Nerodia fasciata pictiventris* (Florida banded water snake) and *Elaphe obsoleta quadrivittata* (yellow rat snake) were chosen because their segmental muscle lengths and numbers of body vertebrae are representative of nonconstricting and constricting colubroids, respectively (Jayne, '82). The aquatic and terrestrial lateral undulation of these two taxa were compared primarily to determine the effects of different numbers of body vertebrae (*Elaphe* 240 vs. *Nerodia* 125) when segmental lengths of major axial muscle segments are similar. Because of the larger number of vertebrae, one would predict that *Elaphe* would be a more flexible animal. Within both of these species, aquatic and terrestrial lateral undulation were studied to clarify the distinctions between these two seemingly similar modes.



## MATERIALS AND METHODS

Species of colubrid snakes were selected either because of the ability of a species to perform a desired locomotor mode or because the kinematics of locomotion had been previously documented for the species (Jayne, '85, '86). The primary species studied were *Nerodia fasciata pictiventris* and *Elaphe obsoleta quadrivittata*. Specimens were obtained from commercial suppliers in southern Florida. The largest individuals of each species were chosen to facilitate electrode placement. Six *N. fasciata* and four *E. obsoleta* snakes were used in this study, and Table 1 summarizes the lengths and masses of those specifically mentioned in this text.

Substrates were chosen that best elicited a particular locomotor mode. Table 1 summarizes the substrates used for particular individuals. A tempered peg board with rotating glass pegs proved most effective for eliciting terrestrial lateral undulation and preventing transitional locomotor modes from being performed. The pegs were placed in square arrays with a spacing of 7.5, 10, or 15 cm between their centers. A pool 1.6 × 4 m with water depth of about 20 cm was used for filming aquatic lateral undulation. These filming areas were sufficiently large to allow snakes to perform a few cycles of movement before and after the time during which they were in the field of view of the camera. Snakes were filmed moving at ambient room temperature (24–28°C).

After being filmed, the snakes were killed with an injection of sodium pentabarbitol. Snout-vent (SV) and tail lengths then were measured to the nearest centimeter, and mass was determined to the nearest gram. For snakes that had been filmed swimming, midsagittal area to the nearest square centimeter was calculated from measurements of the mid-dorsal to mid-ventral heights of the relaxed snake, taken at intervals of 10% of its total length. Snakes were then fixed in 10% formalin and stored in 70% ethanol.

The electrodes used for electromyography were made of .05-mm-diameter, poly-coated, stainless steel wire. A cyanoacrylate glue was used to bond together about the first 10 cm of the strands of each bipolar electrode. With the aid of a dissecting microscope, a razor blade was used to scrape the insulation from the first 0.8–1.2 mm of the electrode wire. The bipolar electrodes were inserted through the skin and into muscles using hypodermic needles. A unipolar ground wire was implanted lateral to the ribs. During early attempts to implant electrodes with 25-gauge needles, snakes were anesthetized with a mixture of halothane and nitrous oxide. This procedure was abandoned after discovery that manual restraint of the snake and implantation with 26-gauge needles gave better results. After insertion, the electrode wires were glued to the skin of the snake with a cyanoacrylate glue with a viscous formula (advertised for bonding leather and wood). Small pieces of plastic were pressed against the glue to facilitate strong bonding. Plastic cement then was used to glue together the two strands of each electrode and to bond the electrodes to each other to form a single cable that was glued to the back of the snake. The lengths of electrode wire from the snake to the probes of the polygraph ranged from 1.5 to 3.0 m, averaging about 2 m. Lengths of wire were used that allowed unimpeded locomotion by the snakes. The number of electrodes implanted in a single snake ranged from four to ten.

Results were used only from electrodes whose positions were determined by dissection of the preserved specimens. Preliminary experiments revealed that different onset and offset could be detected from electrodes in homologous muscle segments that were within three vertebrae of each other. Preliminary analysis also indicated that consistent correlations between kinematic variables and muscle activity oc-

curred only for the vertebrae nearest the contractile tissue of the muscle segment containing the electrode. Consequently, kinematic profiles will be presented only for vertebrae that were adjacent to the belly of the muscle containing the electrode.

The electromyograms (EMGs) were processed by a Grass model 7D polygraph with wide band EEG alternating current amplifiers (models 7P5B and 7P3B). EMGs were not integrated. Low and high filter settings were 10 Hz and 40 kHz, respectively. A 60-Hz filter was also used to minimize noise. Depending on the availability of equipment, EMGs were recorded from four to six muscles simultaneously. The sensitivities of the preamplifiers varied from 50 to 300 uV/cm. The amplified signals were recorded on magnetic tape at 15 i.p.s. with a Honeywell model 5600 eight-channel tape recorder.

EMGs were played back from the tape recorder at 15/16 or 1 7/8 i.p.s. to the pens of the polygraph to provide a paper copy of the signals for which the mechanical response of the pens did not limit frequency response. Select sequences of EMGs, including those shown in the figures, were filtered with a 100-Hz high band pass filter before being played through a Gould model 220 pen recorder. These EMG records were analyzed only for the onset and offset of muscle activity (to nearest .01 sec).

To facilitate certain comparisons among different individuals and sequences, onset and offset of EMGs were converted to a relative time scale, where the duration of a standardized cycle of lateral vertebral flexion was 100%. For this standardized cycle, the vertebrae were straight at 0%, 50%, and 100%. With respect to the side of the snake containing the muscle under consideration, maximal extension (convexity) and maximal flexion (concavity) occurred at relative times of 25% and 75%, respectively. Hence, the vertebrae were being flexed between the relative times of 25% and 75%. The relative duration of muscle activity was calculated by the difference between the relative times of onset and offset. The PC + version of SPSS was used to perform analyses of variance (ANOVA) on the relative duration and times of onset and offset of muscle activity. For one-way ANOVA, Tukey's procedure was used to determine which groups were different. A value of $P$ less than .01 was used in the decision-making criterion for significance.

A Bolex H16 movie camera operated at 50 f.p.s. with a shutter speed of 1/300 sec was used to obtain 16-mm black and white films of snakes. The camera was always positioned vertically above the surfaces on which the snakes crawled. Within view of the camera, a light blinked every half second and simultaneously sent a signal to the tape recorder to insure synchronization of the film and EMG records.

Films were projected with a Lafayette stop-action projector. At regular time intervals, tracings were made of paint marks along the mid-dorsal scales of the snakes. For each resulting tracing, lines about 4 cm long were drawn at the anterior portion of a traced paint mark and tangent to the curve formed by the paint marks representing the vertebrae (Fig. 1). These modified tracings then were digitized with a graphics tablet interfaced to an Apple II+ microcomputer. Each tangentially constructed line on the tracings was digitized by entering its two endpoints. Thus, the more anterior endpoint of each line represented a single point on the moving snake, which allowed determination of linear displacement for this region of the snake. Each pair of endpoints was used to generate the equation of the tangential line, allowing calculation of angular displacement relative to adjacent tangential lines (representing vertebrae). In this way, a record of angular and linear displacements through time was generated for several vertebrae along each snake. Angles between the tangential lines were divided by the number of intervening vertebral joints to calculate mean lateral vertebral flexion ($\bar{\theta}$) over intervals of every four vertebral joints (Fig. 1). Positive values of $\bar{\theta}$ indicate the vertebral column is concave (flexed) to the animal's right. Tracings were oriented so that the overall direction of travel was in the positive X direction and so that movement to the right was in the positive

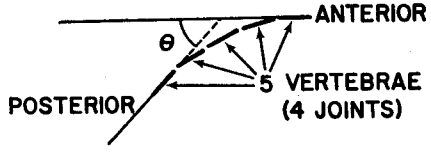


Fig. 1. Method of measuring lateral vertebral flexion from tracings of films; $\bar{\theta} = \theta/4$ = mean lateral vertebral flexion; $\bar{\theta} > 0$ indicates concave (flexed) to the right (R); $\bar{\theta} < 0$ indicates concave to the left (L). Note that this is an example of vertebrae concave to the right.



Y direction (Jayne, '86); hence each overall linear velocity ($V_r$) could be resolved into forward ($V_x$) and lateral ($V_y$) components. After converting all linear velocities to total snake lengths per second, plots of $V_x$, $V_y$, and $V_r$ vs. time were used to determine locomotor mode (Jayne, '86). Muscle activity was superimposed on plots of $\bar{\theta}$, $V_y$, and $V_r$ vs. time to determine the mechanical correlates of EMGs.

## RESULTS

### *Anatomy*

The following descriptions of muscles are based on the average measurements taken from at least three individuals each of *Nerodia fasciata pictiventris* and *Elaphe obsoleta quadrivittata*. Terminology follows that of Gasc ('81). Descriptions are provided only for muscles into which electrodes were implanted rather than for all the axial muscles.

In snakes, the three largest and most superficial longitudinal columns of epaxial muscles are comprised of segments of Mm. semispinalis-spinalis, longissimus dorsi, and iliocostalis. In both *Nerodia fasciata* and *Elaphe obsoleta*, each of the muscular segments of these three muscles receives most muscle fibers from two adjacent vertebral units (e.g., see spinalis origin on vertebrae 17 and 18 in Fig. 2). However, a 1 : 1 correspondence exists between the vertebrae and the following tendinous positions: (1) the long anterior tendon of M. semispinalis-spinalis (AT, Fig. 2), (2) the anterior tendinous arch of M. longissimus dorsi (TA, Fig. 2), and (3) the intermediate tendon between the medial and lateral heads of M. iliocostalis (IT, Fig. 2).

To facilitate comparisons, the vertebra onto which the anterior tendon of a segment of M. semispinalis-spinalis inserted was counted as number 1 and the subsequent vertebrae numbered in posterior sequence. Figure 2 provides a simplified view of the arrangements of the major epaxial muscle segments of *Elaphe obsoleta quadrivittata*. The thin anterior tendon (AT) of the SSP-SP extends posteriorly to end lateral to the 12th vertebra. The muscle tissue of the dorsomedial head (spinalis = SP) of the SSP-SP continues posteriorly for five more vertebrae. The muscle fibers then terminate on the posterior tendons of the segments of the M. multifidus, which extend posteriorly for about two vertebrae and attach to the lateral surface of the neural spine. Thus, the resulting span of vertebrae for one segment of the spinalis is 18, including the vertebrae of origin and insertion. Muscle fibers from the ventrolateral head (semispinalis = SSP) of the SSP-SP terminate on a tendinous sheet at the 18th vertebra. Part of this tendinous sheet contributes to an intermuscular septum (between the SSP-SP and LD). This septum forms a diffuse connection to the vertebra in the region of the prezygapophysis. Another portion of the tendinous sheet extends ventrolaterally to form the medial tendon of the M. longissimus dorsi.

In *Elaphe obsoleta*, muscle tissue from a single segment of the LD extends anteriorly from its origin on the 27th vertebra to insert into a tendinous arch (TA) lateral to the 22nd vertebra. The tendinous arch gives rise to a dorsomedial tendon (MT) that connects with the semispinalis and a ventrolateral tendon (LT) that connects with the medial head of M. iliocostalis. The lateral and medial heads of the IC are connected by an intermediate tendon (IT) that is less than one vertebra long; this tendon lies lateral to the 15th vertebra. The muscle tissue of one segment of the IC, including the intermediate tendon,

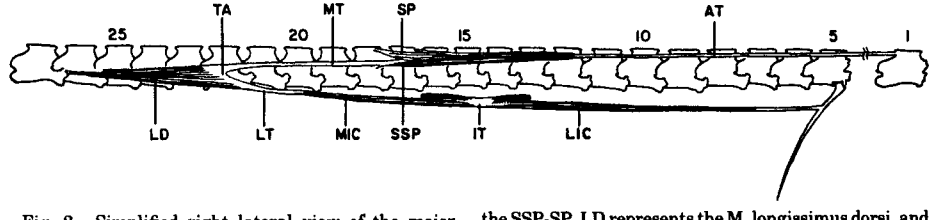


Fig. 2. Simplified right lateral view of the major epaxial muscle segments of *Elaphe obsoleta quadrivittata*. Anterior is to the right. SP and SSP, respectively, indicate the spinalis and semispinalis portions of the M. semispinalis-spinalis, and AT is the anterior tendon of the SSP-SP. LD represents the M. longissimus dorsi, and MT, TA, and LT are the medial tendon, tendinous arch, and lateral tendon of LD. MIC and LIC, respectively, are the medial and lateral heads of the M. iliocostalis, and IT is its intermediate tendon.

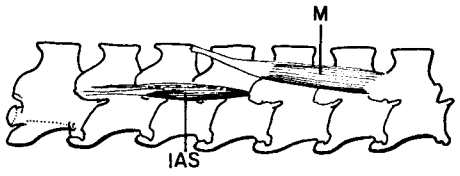


Fig. 3. Simplified right lateral view of deeper epaxial muscle segments of *Nerodia fasciata pictiventris*. Anterior is to the right. The M. semispinalis-spinalis has been removed. The M. multifidus and M. interarticularis superior are abbreviated M and IAS, respectively.

extends anteriorly from the 20th to the seventh vertebra. The tendon from the lateral head extends anteriorly until it attaches to the rib of the fifth vertebra. Hence a single unit of the LD-IC spans 23 vertebrae.

The arrangement of major epaxial muscles of *Nerodia fasciata* (Fig. 2; Jayne, '85) is very similar to that of *Elaphe obsoleta*. The anterior tendon (AT) of the SSP-SP extends posteriorly to end lateral to the 14th vertebra, and the muscle tissue of the spinalis continues posteriorly to the level of vertebra 19. The muscle fibers then terminate on the posterior tendons of the segments of the M. multifidus, which extend posteriorly for one or two additional vertebrae. A single unit of the SP therefore spans 20 vertebrae. In *N. fasciata*, muscle fibers from the SSP terminate on a tendinous sheet at the 20th vertebra, as they do in *Elaphe obsoleta*. In *N. fasciata*, muscle tissue from a single segment of the LD extends anteriorly from the 30th to the 24th vertebra. The origin, insertion, and intermediate tendon of the IC are similar in the two species. The muscle tissue of one segment of the IC extends anteriorly from the 20th to the tenth vertebra of *N. fasciata*, and the tendon from the lateral head extends anteriorly until it attaches to the rib of the eighth vertebra. Thus, a single unit of its LD-IC spans 23 vertebrae.

The following deeper muscles occasionally were implanted with electrodes. The triangular Mm. multifidus (M) of these two species are nearly identical and lie deep to the spinalis (Fig. 3). Anteriorly, the fibers attach widely to the posterior portion of the postzygapophysial wing and taper posteriorly to join a triangular tendon. A complete segment spans five vertebrae.

M. interarticularis superior (IAS = M. diagasticus of Mosauer, '35) is also similar in these two taxa (Fig. 3). Fibers originate from the posterior margin of the postzygapophysis just ventral to the fibers of M. multifidus, extend posteriorly, and bifurcate to form two distinct spindle-shaped heads, each of which attaches to the posterior portion of the postzygapophysis through thin tendons about one vertebra long. Including the surfaces of origin and insertion, four vertebrae are spanned by this muscle.

In *Elaphe obsoleta*, M. interarticularis inferior (IAI) lies deep to the LD, extending anteriorly four vertebrae from its origin on the prezygapophysial process to its insertion on the most proximal portion of a rib. The muscle receives some fibers from each of the vertebrae it spans.

In graphic summaries of results, electrode position is given in parentheses after the muscle abbreviation. It is defined by the most anterior and most posterior vertebrae to which the muscle segment attaches, counting posteriorly from the skull. If an electrode contacted more than one adjacent muscle segment, the span includes the most anterior and posterior origins and insertions of all the contractile tissue of serial homologs containing the uninsulated electrode wire. The designation SSP-SP indicates that the electrode was in the SSP-SP anterior to the bifurcation of the SP and SSP. Span of the IC of *Nerodia fasciata* and *Elaphe obsoleta* includes the associated segmental length of LD.

### *Terrestrial lateral undulation*

Figures 4 and 5 illustrate movement and EMG records for the terrestrial lateral undulation of *Nerodia* 35 crawling through a square array of rotating glass pegs spaced 10 cm apart. Figure 4 shows the EMGs from segments of the SP, LD, and IC from the right side of the snake near midbody. In this figure, mean lateral vertebral flexion ($\bar{\theta}$) was calculated for the four joints between veretbrae 69 and 73. In all similar figures that follow, the linear velocities ($V_y$; $V_r$) are shown for the most anterior vertebra of the body segments used to determine $\bar{\theta}$ (e.g., vertebra 69 in Fig. 4). For this sequence, the overall mean $V_x$ from 0 to 3.26 sec was 0.29 total lengths (TL)/sec. For the same time interval, the coefficient of variation (CV) of $V_r$ was a rather small 21%, indicating that the snake was not combining lateral undulation with other modes (see Jayne, '86 for more detail on use of these quantities for determining locomotor mode). Two complete periods of



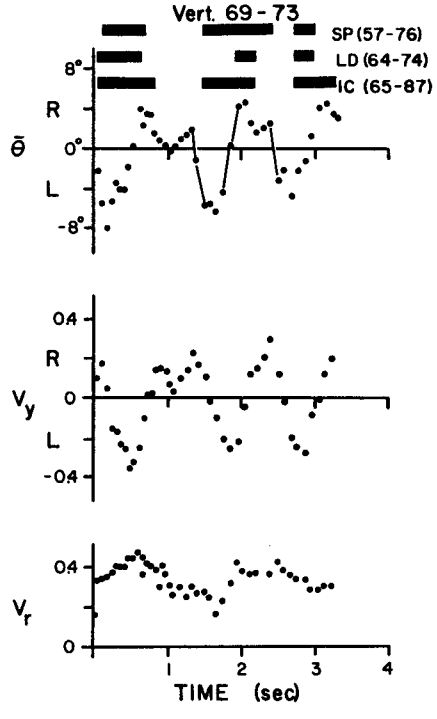


Fig. 4. Simultaneous EMG and movement records from of *Nerodia* 35 performing terrestrial lateral undulation with 10-cm peg spacing. Right and left are abbreviated R and L. Oblique lines connecting dots are only to facilitate recognition of successive points in time. Numbers in parentheses after muscle abbreviations indicate the vertebrae spanned by the muscle segments containing the electrodes. Horizontal bars represent EMG. EMGs of muscles from the right side of the snake are diagrammed above the portion of the plot of $\bar{\theta}$ indicating lateral vertebral flexion concave to the right. Velocities are in TL/sec and are for the first vertebra (69) in the interval used to determine $\bar{\theta}$. $V_r$ is overall speed and $V_y$ is the lateral component of $V_r$.

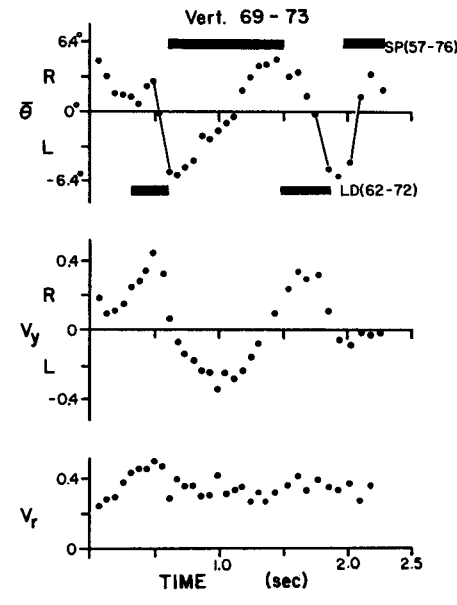


Fig. 5. Simultaneous EMG and movement records from *Nerodia* 35 performing terrestrial lateral undulation with 10-cm peg spacing. Notation as in Fig. 4.

motion were evident from 0.62 to 2.05 and from 2.05 to 3.15 sec, and means of $V_x$ for these time intervals were 0.28 and 0.30 TL/sec, respectively. The three cycles of activity of the right-side segments of the SP, LD, and IC began when vertebrae 69–73 were maximally flexed to the left (convex to the right) and ended when these vertebrae were maximally concave to the right. These three muscles were generally active in synchrony at any given longitudinal position of the body.

The value of $\theta$ does not show a perfect sinusoidal function with time. Instead, the first two flexions to the right showed decreases roughly midway through flexion to the right. These momentary decreases in right-side flexion were caused by the snake forming a rather low amplitude–long wavelength flexion to the right. In other words, the crest of this half wave was shallow, with the vertebrae nearly becoming straight as they approached maximum lateral displacement.

Figure 5 shows another sequence of lateral undulation of *Nerodia* 35 and activity from a right-side SP and left-side LD. Mean $V_x$ is 0.27 TL/sec, and CV of $V_r$ is 19% from 0 to 2.10 sec. Mean $V_x$ during the half periods between 0.62, 1.11, 1.77, and 2.10 sec was 0.25, 0.24, and 0.31 TL/sec, respectively. The contractile tissue of these two muscle segments occupied nearly the same longitudinal position along the body of the snake. Muscle fibers of the right SP spanned vertebrae 70–75 and those of the left LD spanned vertebrae 66–72. Almost immediately after the cessation of right-side activity, left-side contraction began. The activity of each side began at the time of maximal convexity and ended at the time of maximal concavity.

*TABLE 1. Measurements of individuals of* Nerodia fasciata *(NF) and* Elaphe obsoleta *(EO) tested during swimming or terrestrial locomotion*[1]

| Snake | Substrate[1] | Sex | Mass (gm) | Length (cm) | | Vertebrae | | Area ($cm^2$)[3] | |
|---|---|---|---|---|---|---|---|---|---|
| | | | | Total | SV[2] | Total | Body | Total | Body |
| NF36 | 7.5-cm pegs | M | 76 | 68 | 48 | 212 | 126 | — | — |
| NF35 | 10-cm pegs | M | 124 | 73 | 52 | 204 | 125 | — | — |
| NF39 | Water | M | 79 | 62 | 47 | 190 | 126 | 75 | 64 |
| NF38 | Water | F | 152 | 73 | 55 | 199 | 129 | 107 | 97 |
| NF34 | Water | F | 260 | 85 | 67 | 171 | 125 | 146 | 138 |
| EO18 | 15-cm pegs | F | 353 | 153 | 118 | 326 | 242 | — | — |
| EO20 | Water | F | 165 | 112 | 91 | 330 | 245 | 146 | 137 |
| EO19 | Water | M | 455 | 149 | 121 | 321 | 235 | 263 | 242 |

[1]For substrate, distances indicate spacing between centers of pegs in square arrays.
[2]SV indicates snout-vent.
[3]All areas are for mid-sagittal projections.

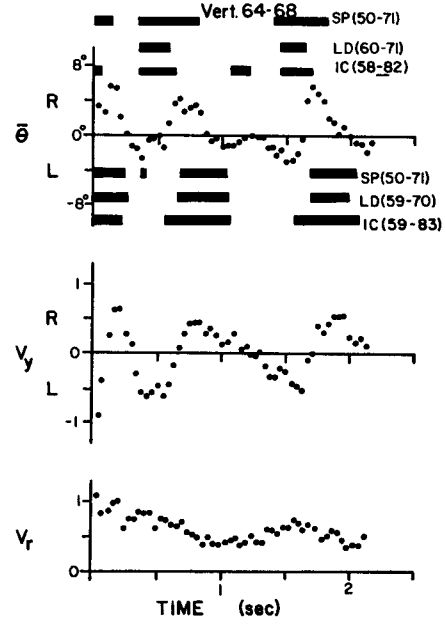


Fig. 6. Simultaneous EMG and movement records from *Nerodia* 36 performing terrestrial lateral undulation with 7.5-cm peg spacing. Notation is as in Fig. 4.

*Nerodia* 35 also performed the slowest sequence of lateral undulation among those analyzed ($V_x$ = 0.07–0.10 TL/sec). As time increased, so did lateral flexion ($\theta$ = 8° at 2.29 sec and 10° at 3.18 sec); hence, the waveform of the snake changed through time. However, the LD near midbody still became active as the region became maximally convex and inactive as the region became maximally concave.

Figure 6 shows EMG and movement records for almost three cycles of activity for the lateral undulation of *Nerodia* 36 moving through pegs spaced 7.5 cm apart. Mean $V_x$ and CV of $V_r$ for the entire sequence were 0.47 TL/sec and 34%, respectively. For the two periods between 0.13, 0.63, and 1.71 sec, the values of mean $V_x$ and CV of $V_r$ were 0.63 TL/sec, 17%, and 0.43 TL/sec, 21%, respectively. Thus, the snake was undulating laterally, although it decelerated significantly during this sequence. The SP, LD, and IC of the same side generally were active synchronously. The left and right LD and IC primarily displayed unilateral activity, whereas the activity of the left and right SP overlapped from 0.66 to 0.82 sec and from 1.69 to 1.84 sec. Left-side activity almost immediately followed right-side activity in all three muscles; however, there was a slight pause (0.34) of most activity between the end of synchronous left-side activity (1.05 sec) until the start of synchronous right-side activity (1.39 sec). During this momentary cessation of synchronous SP, LD, and IC activity, this region of the snake became nearly straight as it formed the crest of a low amplitude–long wavelength lateral flexion. Some activity of the right IC correlated with this slight straightening of the snake's body. Most activity occurred as regions were maximally convex and continued until maximally concave.

Figure 7 illustrates EMG and movement records for the LD and IAS at two sites in *Elaphe* 18 performing lateral undulation past pegs with 15-cm spacing. Near the middle of this sequence, the anterior portion of the snake began to turn left. For the more posterior site (vert. 169), which traveled a slightly straighter path, overall mean $V_x$ and CV of $V_r$ were 0.33 TL/sec and 29%, respectively. For the period from 0.19 to 1.00 sec and the half-period from 1.00 to 1.76 sec, values of mean $V_x$ and CV of $V_r$ were 0.27 TL/sec, 34%, and 0.36 TL/sec, 23%, respectively. Two cycles of muscle activity were observed at each of these sites. For both sites, right-side activity immediately followed left-side activity, but no activity occurred for about 0.5 sec while these regions of the snake were nearly straight (Fig. 7). Allowing for the complication of the momentary straightness of the vertebral column, all four of these muscles became active when their side was maximally convex, and activity ceased when their side was maximally concave. For both sites, the first transition from left to right muscle activity slightly preceded left maximal concavity. However, comparison of activity between the two sites showed transitions of left-to-right muscle activity at comparable positions on the graph of $\theta$ vs. time. In other words, the lag time was the same for muscle activity and for the mechanical response of lateral flexion as these two events traveled posteriorly along the snake.



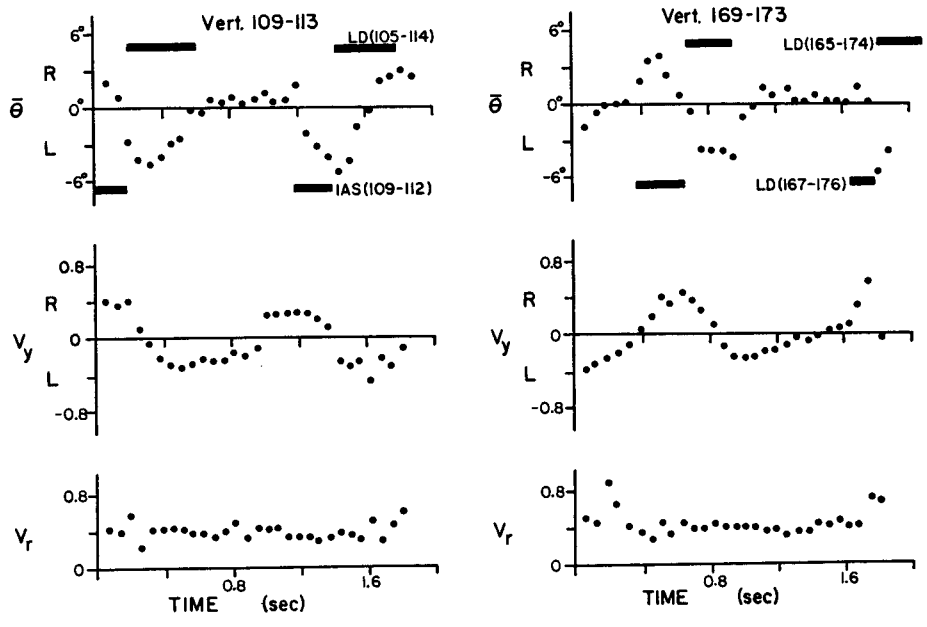


Fig. 7. Simultaneous EMG and movement records from two longitudinal sites of *Elaphe* 18 performing terrestrial lateral undulation with 15-cm peg spacing. Notation is as in Fig. 4.

Two-way ANOVA of the relative time of onset and offset of activity during terrestrial lateral undulation revealed no significant differences, either between *Nerodia* 35 and *Nerodia* 36 or among the SP, LD, and IC muscles. The insignificant interindividual differences allowed pooling of data from NF35 and NF36 to summarize muscle activity during a standardized cycle of lateral vertebral flexion, as shown in Fig. 8. For the pooled relative times of onset and offset (Fig. 8), no significant differences were found among the SP, LD, and IC with one-way ANOVA. As shown in Fig. 8, nearly all activity of these muscles occurred as the vertebrae were laterally flexing toward the side of the active muscle. Muscles were generally active for 50% of a cycle of vertebral flexion (Fig. 8). However, one-way ANOVA of the pooled data (Fig. 8), did reveal that the relative duration of activity of the LD (38%) was slightly less than that of the SP (55%) and the IC (52%).

To summarize, for terrestrial lateral undulation past a limited number of pegs, the

*TABLE 2. Location of electrodes used in swimming snakes, identified by vertebral number (v) and distance from the snout of the snake*

| Snake | Site 1 | Site 2 | Site 3 | Site 4 |
|---|---|---|---|---|
| NF34 | 46 v 25 cm | 70 v 39 cm | 94 v 53 cm | — |
| NF38 | 29 v 12 cm | 64 v 28 cm | — | — |
| NF39 | 30 v 11 cm | 64 v 24 cm | 97 v 39 cm | — |
| EO20 | 76 v 29 cm | 116 v 45 cm | 153 v 60 cm | 192 v 74 cm |
| EO19 | 65 v 32 cm | 119 v 59 cm | 165 v 86 cm | — |

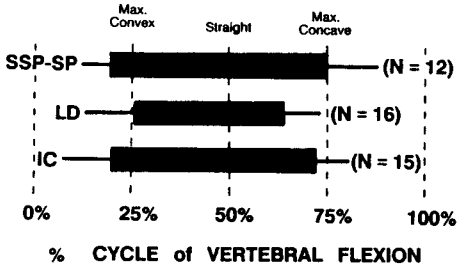


Fig. 8. Mean relative times of onset and offset of muscle activity during the terrestrial locomotion of *Nerodia*. Data were combined from NF35 and NF36. The ends of the thick horizontal bars represent the mean times of onset and offset of activity during a standardized cycle of lateral vertebral flexion. The thin horizontal lines are ± 1 standard deviation. For each bar, abbreviations of muscles and sample sizes are to the left and right, respectively. Note that lateral vertebral flexion toward the side of the active muscle occurs between 25% and 75%.

SSP-SP, LD, and IC started activity whenever their belly was at the site of maximal convexity and ceased activity when the region was maximally concave (Fig. 8). Activity was propagated posteriorly in an alternating, unilateral fashion. These contractions were correlated with further lateral flexion of the more posterior vertebrae toward the side of the active muscle. Movement of snakes without occasional straightenings of the body involved immediate transition of activity between opposite sides of the body.

### *Aquatic lateral undulation*

Snakes swim by propagated waves of lateral flexion whose amplitude, wavelength, and speed increase posteriorly along the snake. The speed of the waves traveling along most of the body is greater than the forward speed of the snake through the water. The snakes used in this study usually swam along the surface of the water with the body held at a slight angle to the surface. The head often was held entirely out of the water, whereas the more posterior portions of the snake remained completely submerged (Jayne, '85). This posture is referred to as normal surface swimming.

Electrodes were usually implanted at three longitudinally displaced positions along the body of the snake, but in one (*Elaphe* 20) there were four such positions. Table 2 lists the locations of the electrodes as confirmed by dissection. These sites are referred to by their site number (Table 2), with numbering proceeding from anterior to posterior.

Figure 9 shows $\bar{\theta}$, $V_y$, and $V_r$ for left-side segments of SSP-SP, SP, and LD near midbody of the largest *Nerodia* (34) and $\bar{\theta}$ for left-side segments of LD at additional sites near 2/5 and 4/5 of the body length. This snake swam normally for the entire sequence. For site 2, mean $V_x$ was 0.81 TL/sec and CV of $V_r$ was 13.6% from 0 to 1.0 sec. For the two half-periods between 0.21, 0.50, and 0.83 sec, mean $V_x$ was 0.85 and 0.67 TL/sec, respectively. The left-side site-1 LD initiated activity when its region was convex to the left, and activity ceased as the region became concave to the left. The site-2 muscles on the left side began contraction when the region was nearly maximally convex to the left and ceased firing about when the region was straight. The left side site-3 LD began contraction when the region was almost straight, continued while the region was convex to the left, and ceased just before the region became straight again. At all three sites, the duration of the EMG burst was slightly less than the interval between bursts. For example, the second contraction of the site-2 LD lasted 0.22 sec, compared to the 0.37 sec of inactivity that preceded it. The plots of $\bar{\theta}$ versus time for the three positions along the snake illustrate the EMG and mechanical waves traveling posteriorly within the body of the snake.

Figure 10 diagrams EMGs and movement of *Nerodia* 34 swimming below the surface



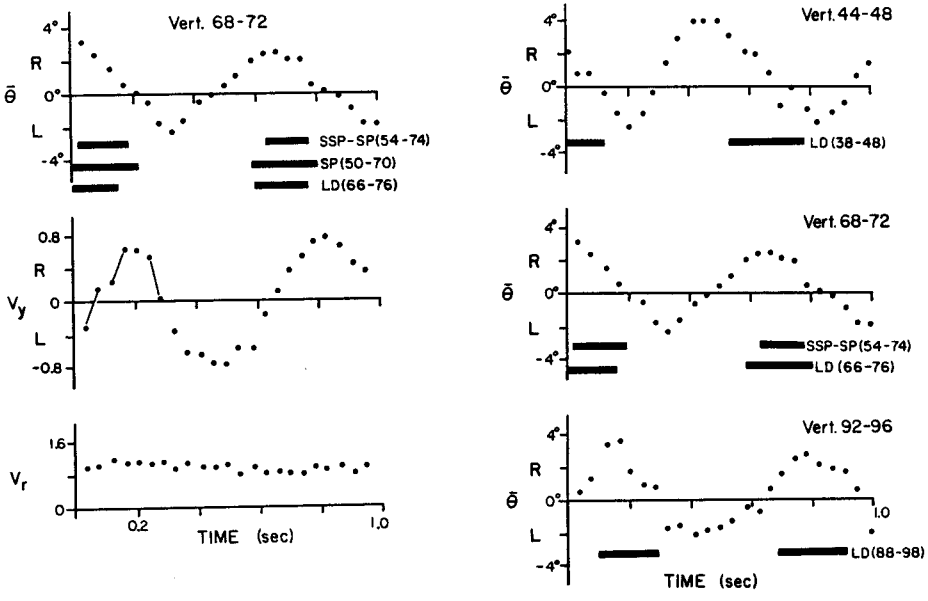


Fig. 9. Simultaneous EMG and movement records from *Nerodia* 34 performing aquatic lateral undulation at the surface of the water. At left, $\bar{\theta}$, $V_y$, and $V_r$ for the site near midbody. At right, $\bar{\theta}$ for three different longitudinal sites. Notation is as in Fig. 4.

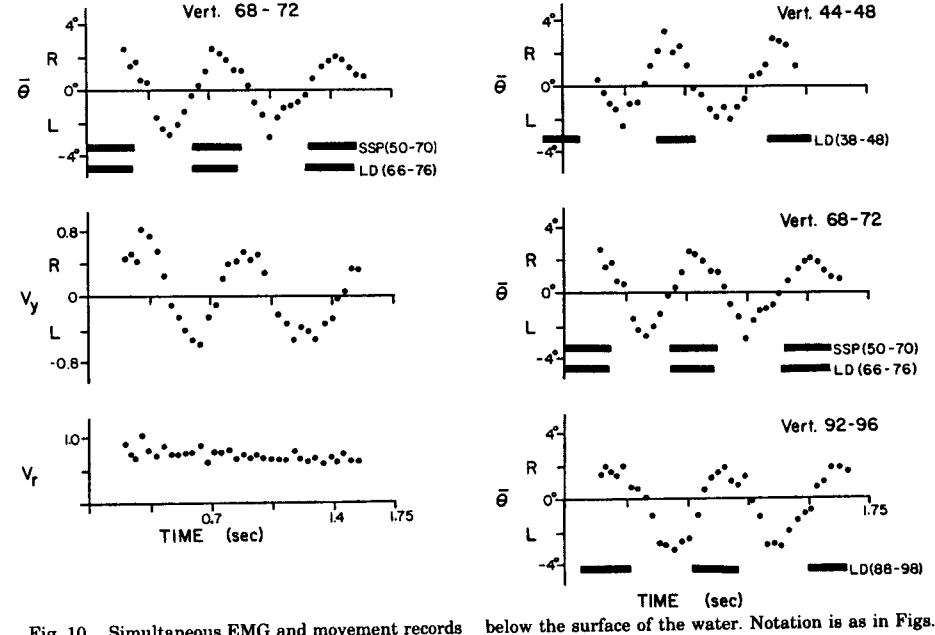


Fig. 10. Simultaneous EMG and movement records from *Nerodia* 34 performing aquatic lateral undulation below the surface of the water. Notation is as in Figs. 4 and 9.

*TABLE 3. Representative maxima and minima of $\bar{\theta}$ (see Fig. 1) for four sequences of undulation in swimming snakes*[1]

| Snake | Site 1 | | Site 2 | | Site 3 | | Site 4 | |
|---|---|---|---|---|---|---|---|---|
| NF34 | −2.4° | (.33) | −2.7° | (.46) | −3.1° | (.63) | — | |
| (submerged) | 3.3° | (.58) | 2.4° | (.84) | 1.9° | (.92) | — | |
| | −2.0° | (.96) | −3.0° | (1.04) | −3.0° | (1.25) | — | |
| NF39 | −3.7° | (.25) | −6.4° | (.42) | −4.7° | (.58) | — | |
| | 3.7° | (.42) | 5.3° | (.58) | 3.1° | (.75) | — | |
| | −3.3° | (.58) | −5.2° | (.79) | −4.5° | (.96) | — | |
| EO20 | — | | — | | 1.8° | (.08) | 0.9° | (.15) |
| | −1.0° | (.04) | −1.7° | (.15) | −1.4° | (.29) | −1.3° | (.38) |
| | 1.5° | (.21) | 1.0° | (.33) | — | | — | |
| EO19 | — | | 0.9° | (.08) | 2.0° | (.29) | — | |
| | −1.7° | (.25) | −1.5° | (.37) | −1.9° | (.54) | — | |
| | 1.3° | (.37) | 1.9° | (.58) | — | | — | |

[1]For each electrode site, values in parentheses after each angle indicate the time in seconds when this angle occurred during these illustrated sequences; angles are listed so that reading a row from left to right enables one to follow a half wave through time as it travels posteriorly along the body of the snake.

of the water throughout the sequence. In this interesting trial, the entire length of the snake was submerged with the head deepest below the surface, while the most posterior 20 cm of the snake were close enough to the surface to cause ripples in the water. For site 2 between 0.23, 0.84, and 1.50 sec, two cycles of movement occurred, with values for mean $V_x$ and CV of $V_r$ 0.64 TL/sec, 12%, and 0.56 TL/sec, 7%, respectively. Within each of the three sites, the relation of the EMG to $\bar{\theta}$ remained constant through time. The site-1 LD from the left side began activity at the time the region was maximally convex to the left and ceased before the region became maximally concave to the left. The muscles of sites 2 and 3 were mostly active when these regions were convex to the left. Table 3 lists values of the maximal lateral flexion attained at each of the three sites of *Nerodia* 34. For this snake, adjacent vertebrae flexed laterally less than 3.5°, and values of $\bar{\theta}$ did not vary among the three sites.

Comparing the surface and submerged swimming of NF34 (Fig. 9 vs. Fig. 10), the relative time of onset of muscle activity at all three sites during submerged swimming occurred an average of 16% of a standardized cycle earlier. A two-way ANOVA of the relative times of activity verified that there was a significant effect of being submerged and that there were significant differences among the three sites. The differences among sites, for both surface and submerged swimming, were the result of the relative time of onset of activity occurring progressively earlier for more posterior sites.

Figure 11 illustrates movements and EMGs recorded from *Nerodia fasciata* 39 swimming rapidly on the surface of the water. This snake displayed typical waveform for its size, but the angle between the surface of the water and the plane containing the snake was larger (18°) than the normal value of 5° (Jayne, '85). The swimming of this snake otherwise appeared normal, and this particular snake swam in a straight path, allowing several cycles to be observed. Even though the value for CV of $V_r$ was only 22% for 0.08 to 0.92 sec, the snake did decelerate from 0.13 to 0.79 sec, as indicated by the mean values of $V_x$ for the four half-periods during this interval (1.16, 0.90, 0.87, and 0.74 TL/sec, respectively). The EMGs were primarily unilateral; the only exception was some the weak activity of the right M segment at site 1. The change of the EMG relative to $\bar{\theta}$ along the body of the snake was similar to that of other *N. fasciata*, and this resulted in significant differences in the relative time of onset of activity among the three sites (one-way ANOVA).

Figure 12 illustrates sample EMGs from four muscles in NF39. A consistent decrease in amplitude and increase in the duration of the EMG bursts was seen as the snake decelerated. Over the time interval of each EMG of this sequence, mean $V_x$ was calculated for each point on the body nearest the electrode. Excluding the M. multifidus after 0.2 sec, the duration of muscle activity varied from 0.08 to 0.26 sec ($\bar{x}$ = 0.159, SD = 0.0459, N = 16), and mean $V_x$ varied from 0.57 to 1.23 TL/sec. Duration of EMG



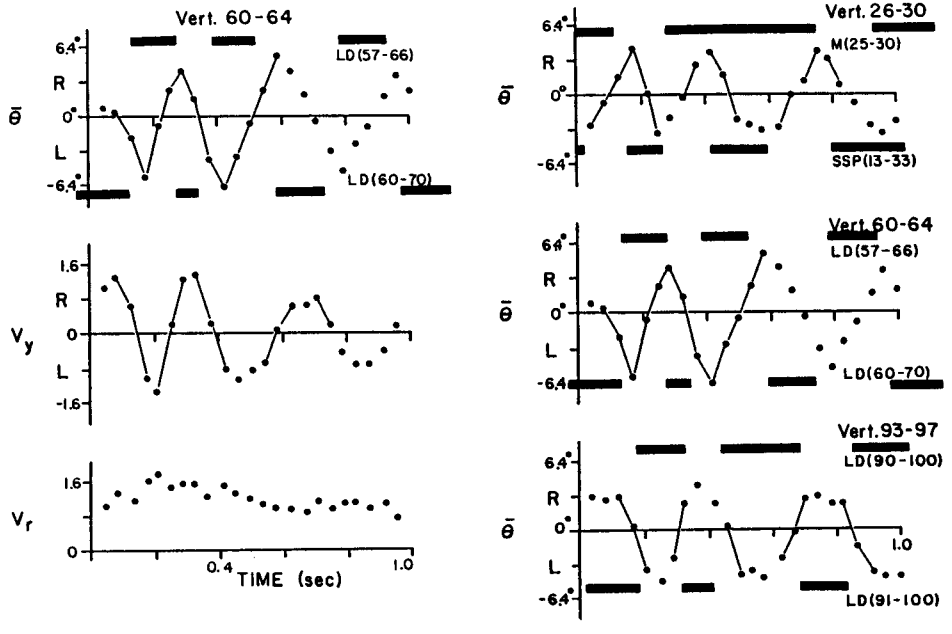


Fig. 11. Simultaneous EMG and movement records from *Nerodia* 39 performing aquatic lateral undulation at the surface of the water. Notation is as in Figs. 4 and 9.

correlated negatively ($P < .05$, $r = -.527$) with mean $V_x$.

Another interesting aspect of this sequence was a consistent difference in the maximum lateral vertebral flexion along the length of the snake (Table 3). For a given wave traveling posteriorly along the body, the flexion at site 2 consistently exceeded that of sites 1 and 3. The greatest flexions observed at sites 1 through 3 were 4.2°, 6.4°, and 4.8°, respectively.

Figure 13 illustrates the movements and muscle activity of the smaller of the two specimens of *Elaphe obsoleta* that were filmed swimming. EO20 used a normal posture relative to the surface of the water as it swam, but it seemed to use a wave of bending with small lateral displacement, compared with that of other *Elaphe* individuals. However, this was consistently characteristic of the swimming of EO20 rather than just a peculiarity of this sequence. Two half-periods of movement occurred between 0.04, 0.23, and 0.42 sec, and the snake maintained very uniform forward and overall speeds, as indicated by site 2 values of mean $V_x$ and CV of $V_r$ of 0.63 TL/sec, 13%, and 0.63 TL/sec, 14%, for the two half-periods, respectively. Although the maximal values of lateral vertebral flexion were small compared with those of *Nerodia fasciata* (Table 3), *Elaphe* 20 and *N. fasciata* showed similar relations between the EMGs and $\bar{\theta}$. Anteriorly, muscles were active during the transition from convex to concave, and convex-region activity predominated posteriorly. The ipsilateral EMGs of each pair of adjacent sites overlapped substantially, indicating more than 40 adjacent muscle segments were active simultaneously. Figure 14 illustrates sample EMGs from EO20 during this sequence and clearly shows the phase lag that occurred as the muscle activity was propagated posteriorly.

Figure 15 diagrams the movements and EMGs for the larger *Elaphe obsoleta* (EO19). This snake swam normally at the surface, swimming with mean $V_x$ of 0.78 TL/sec and CV of $V_r$ of 9% over the three half-periods occurring from 0.04 to 0.62 sec. Despite the difference in size and speed of snakes for the illustrated sequences of EO19 and EO20, the

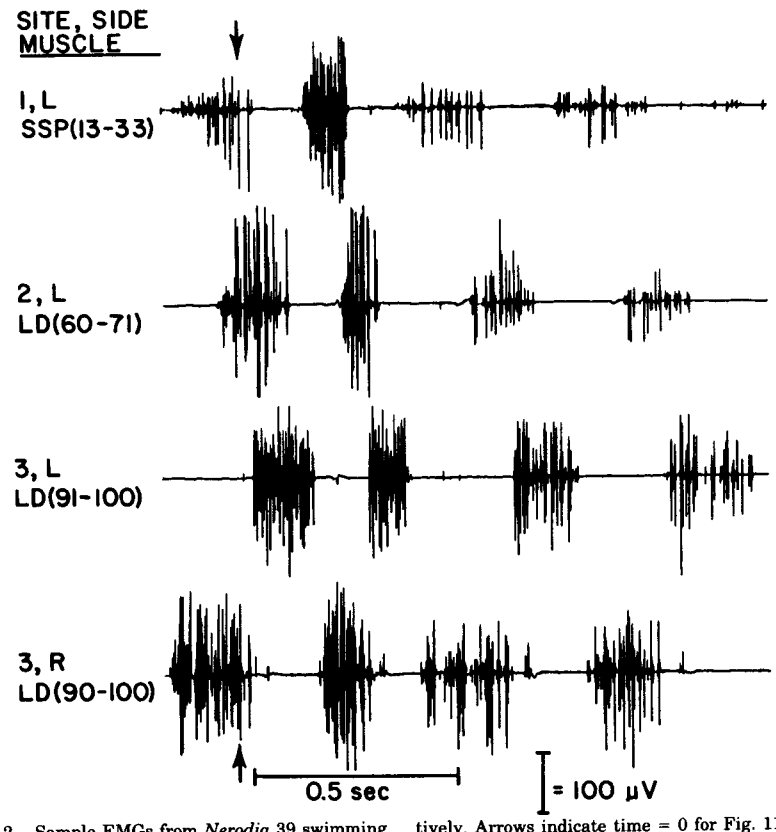


Fig. 12. Sample EMGs from *Nerodia* 39 swimming with highly variable forward velocity. Horizontal and vertical lines indicate time and voltage scales, respectively. Arrows indicate time = 0 for Fig. 11. Note the decrease in EMG amplitude and increase in duration as velocity decreases.

EMGs have a similar relation to $\bar{\theta}$ along the length of the snakes. In contrast to EO20, the EMGs of EO19 usually were as long as the periods of inactivity between them. The activity of the left and right side muscles overlapped slightly at site 2. Most of this overlap occurred during the later portion of the right SSP and the early portion of the left SSP. Two-way ANOVA comparing the relative times of onset and offset detected no significant differences between EO20 and EO19, whereas site location did have a significant effect.

In all swimming snakes, the lag of muscular and mechanical waves changed as they moved posteriorly along the snakes. For each snake, mechanical lag (in seconds) was determined between adjacent sites by maximal, minimal, and zero $\bar{\theta}$, and this factor was compared with corresponding onsets and offsets of EMGs. All resulting phase lags for each pair of adjacent sites were averaged for an entire sequence.

The mean phase lags of EMGs and mechanical events are listed in Table 4. For a given pair of adjacent sites within a single snake during a single sequence, the phase of the EMG almost always lagged less than the mechanical event. In other words, the EMG wave consistently traveled faster than the mechanical wave within the body of the snake. Furthermore, the usual posterior decrease in EMG phase lag indicates that the velocities of the EMG waves generally increased posteriorly along the body of the snake.



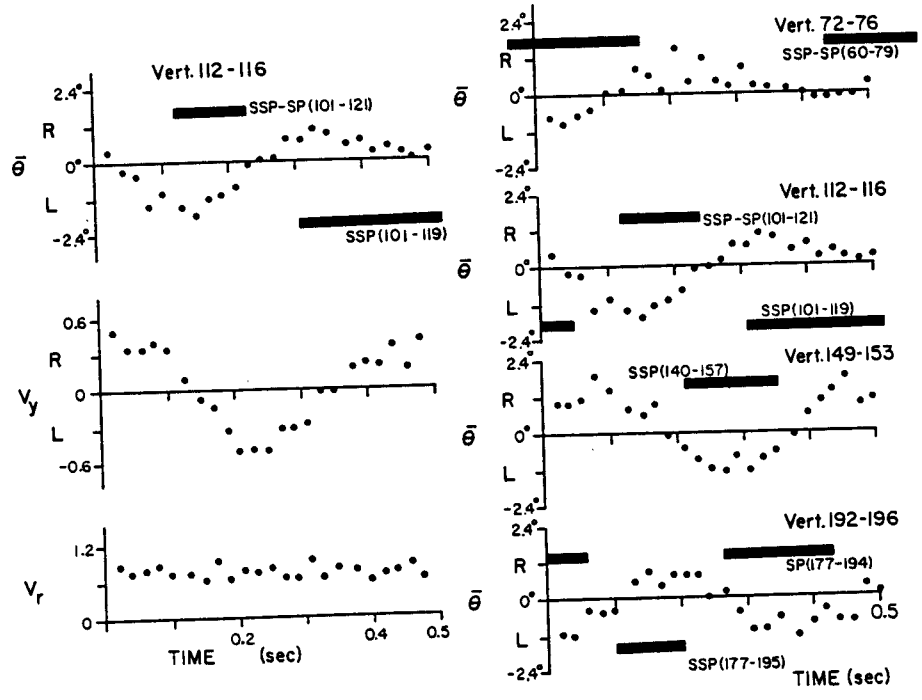


Fig. 13. Simultaneous EMG and movement records from *Elaphe* 20 performing aquatic lateral undulation at the surface of the water. At left, $\bar{\theta}$, $V_y$, and $V_r$ for the site near midbody. At right, $\bar{\theta}$ for four different longitudinal sites. Notation is as in Figs. 4 and 9.

Figure 16 summarizes some of the relative times of onset and offset of muscle activity of the three *Nerodia* and two *Elaphe*. For surface swimming, one-way ANOVA of the relative time of onset at the midbody site revealed significant differences among the three *Nerodia*. In light of this significant interindividual variation, it was not surprising that one-way ANOVA (with individuals nested within species) did not detect significant differences in the relative time of muscle activity between *Nerodia* and *Elaphe*, at a given site.

In summary, snakes swam by alternating, posteriorly propagated unilateral muscle contractions. Anteriorly, the muscles were active during the transition from convex to concave on the side of the active muscle. However, this relation of EMG to mechanical event changed posteriorly because the EMG wave was traveling faster than the mechanical wave within the body of the snake.

## DISCUSSION

### *Evaluation of models*

The only explicit predictions of a muscular mechanism of snake locomotion are the models of lateral undulation proposed by Gray and Lissmann ('50) and Gray ('53). All of these models describe patterns of unilateral muscle activity that would allow snakes to perform lateral undulation for such conditions as a channel with rectangular bends, various numbers of pegs, or water. Two key predictions of the models involve the relationships of muscle activity to the substrate and to the patterns of flexion occurring within the body of the snake.

Gray and Lissmann ('50) used two experimental chambers to quantify forces involved in lateral undulation. In one experiment where snakes crawled through a channel with a series of right angle bends, they determined that forces were applied only to the alternate sides of the channel that

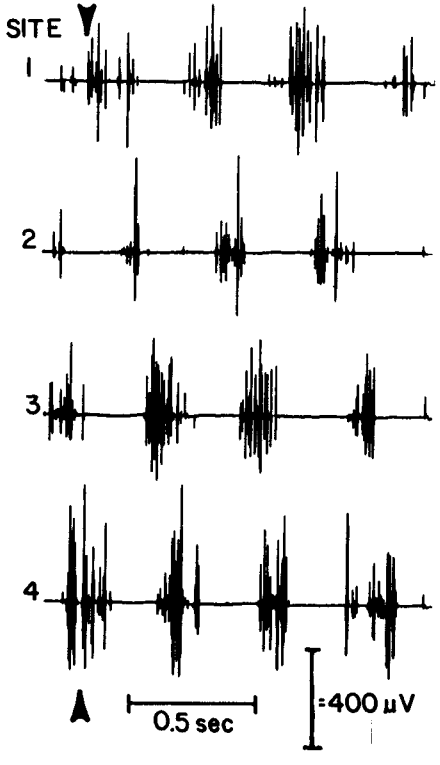


Fig. 14. Sample EMGs from the right side of *Elaphe* 20 swimming with nearly constant forward velocity. Notation is as in Fig. 12. Sites 1–4 were 29, 45, 60, and 70 cm, respectively, from the snout of the snake. Electrodes 1–4 were in contractile tissue near vertebrae 73, 116, 153, and 192, respectively. Note that the overlap of activity between sites 3 and 4 is greater than that of sites 1 and 2.

faced anteriorly. Assuming the entire lengths of a snake between bends of a channel act as a lever arms and that muscles are contractile elements joining adjacent lever arms, Gray and Lissmann predicted that the pattern of muscular effort shown in Fig. 17D was consistent with the observed forces. Despite the equal spacing of bends in the body of the snake, the regions of simultaneously active muscle are not of equal length. This model predicts muscle activity that may or may not be constant with respect to the substrate (see Fig. 17D, bends 3 and 4 vs. bend 2), and activity does not show a constant relationship to the mechanical event of flexion within the body of the snake.

In a second experiment, Gray and Lissmann ('50) allowed snakes to crawl past a series of pendulums the displacement of which indicated the resultant forces applied by the snake performing lateral undulation. The forces generated by the snake always were directed posterolaterally relative to the snake. The resulting reactive forces were directed anteromedially. When the reactive forces at each pendulum were resolved into forward and lateral components, Gray and Lissmann found that the sum of the lateral components approximated zero, resulting in a net forward reactive force that propelled the snake.

Gray and Lissmann ('50) also considered the muscular mechanisms of hypothetical snakes crawling past various numbers of rigid pegs (Fig. 17A–C). In the models, the pegs usually are located on the concave side of the snake at regions of maximum lateral displacement. Figure 17C illustrates part of Gray and Lissmann's model of a snake crawling past three to four pegs. If the regions of active muscle travel posteriorly in the snake, then the cycle of movement of a particular segment can be predicted by examining the posture of the body from posterior to anterior within a block of contracting muscle. For example, with the activity shown at time ii, a segment on the left side should go through phases of straight, convex, straight, and finally concave as peg 4 is passed. At different times (some not shown in Fig. 17C), the transition from left- to right-side activity occurs at regions that are concave right, straight, or concave left. The muscle contractions predicted from this model do not show a constant relationship to the location of pegs (see peg 3) or to the patterns of flexion occurring within the body of the snake.

When Gray ('53) reviewed the general properties of undulatory propulsion, he suggested that the general properties of undulatory swimming and terrestrial locomotion were the same, except that the wave of bending travels faster than the forward speed of the swimming animal. Gray proposed the model of a muscular mechanism shown in Fig. 17E. Although Gray discussed mainly swimming, he included symbols to represent the pattern of external resistive forces. The mechanism consists of alternating, posteriorly propagated unilateral contractions. Activity begins when a region is maximally convex and continues until the region is



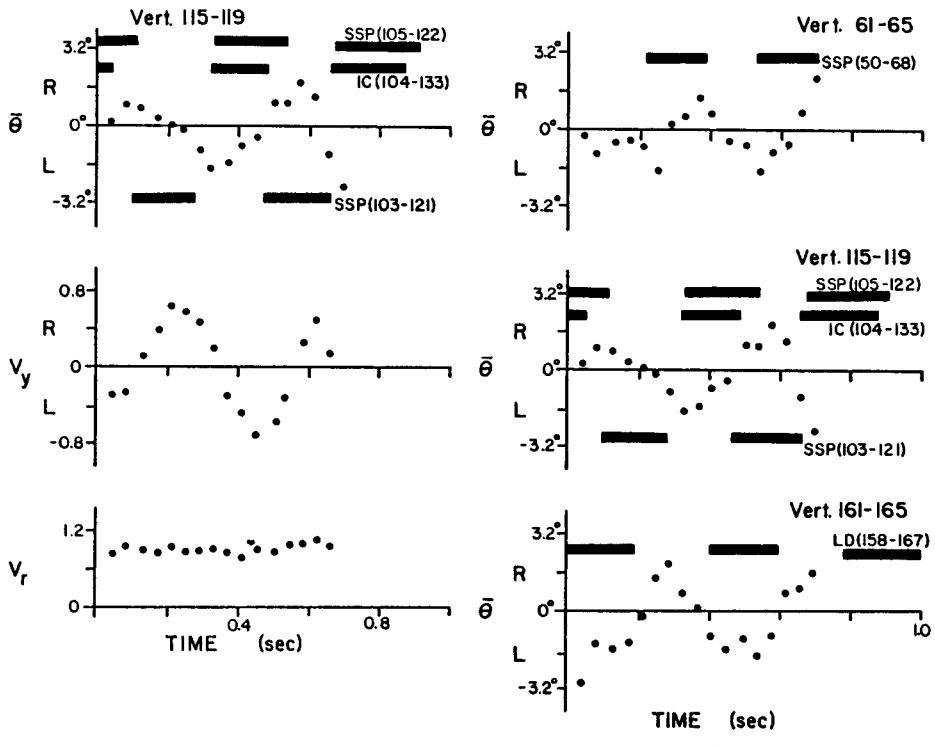


Fig. 15. Simultaneous EMG and movement records from *Elaphe* 19 performing aquatic lateral undulation at the surface of the water. At left, $\bar{\theta}$, $V_y$, and $V_r$ for the site near midbody; at right, $\bar{\theta}$ for three different longitudinal sites. Notation is as in Figs. 4 and 9.

maximally concave, and the greatest tension is generated midway through this cycle (Fig. 17E).

Thus, three primary models of the muscular mechanism of lateral undulation were proposed by Gray and his co-workers. Common to all three is the posterior propagation of alternating, unilateral contractions of muscles, each of which is assumed to span only one body segment. The model of Gray ('53) shows a constant relationship of muscle activity to mechanical events within the body of the organism, with contractions occurring from maximal convexity to maximal concavity (Fig. 17E). The model of a snake moving through a channel with rectangular bends (Gray and Lissmann, '50) shows some consistency between muscle activity and the substrate, and most contractions include a cycle of straight, concave, and straight (Fig. 17D). The model for snakes moving past rigid pegs (Gray and Lissmann, '50) shows no consistent relationship between muscle activity and either the substrate or events within the body of the snake (Fig. 17A–C). In a later review of animal locomotion (Gray, '68), these contradictions were not discussed.

In this study, electromyography of terrestrial lateral undulation was conducted with snakes crawling past fixed pegs, and Fig. 18A illustrates a working model of this case. For the snakes in this study, muscle activity began at maximal convexity and ceased at maximal concavity on the side of the active muscle (Fig. 8). This relation of EMG to mechanical event remained constant along the length of the snake. Muscle contractions were also alternating, unilateral, and propagated posteriorly (Figs. 4–7, 18A). This finding supports Gray's ('53) model of lateral undulation, shown in Figure 17E. Surprisingly, the least applicable model was the one

for a snake moving past a minimal number of rigid pegs (Gray and Lissmann, '50). An important factor affecting this model may be the choice of snake postures for the analysis of forces. The pegs in these models were always located on the concave side of the snake at regions of maximum lateral displacement (Fig. 17A–C). Figure 19 illustrates representative postures of snakes moving past minimal numbers of pegs. These figures are from tracings of films from Gray and Lissmann ('50) and from this study. In contrast to their model, pegs were consistently located about midway between regions of maximal lateral displacement. Gans ('74) stressed the need of anteromedially directed surfaces for snakes to generate the reactive forces necessary for lateral undulation. Here, medial is considered to be located toward the line bisecting distances between successive points of maximum lateral displacement (= overall direction of travel). The posture of the snake contacting pegs in Gray and Lissmann's ('50) model is not consistent with this requirement (see Fig. 17A–C), whereas the posture of the snake in the channel with bends is (Fig. 17D). Perhaps this accounts for the intermediate accuracy of predictions from the model of the snake in the channel with bends.

Gray and Lissmann ('50) often predicted that the muscles were active throughout the

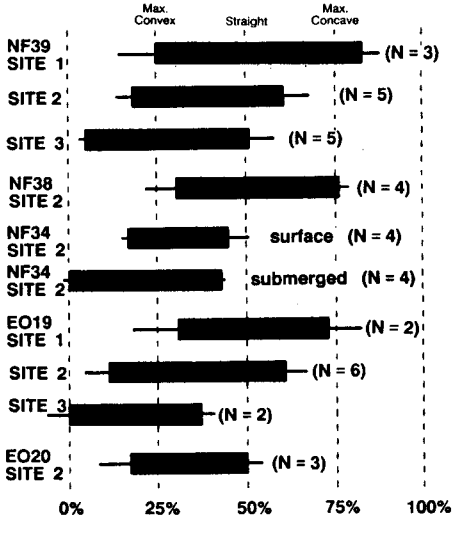


Fig. 16. Mean relative times of onset and offset of muscle activity during aquatic lateral undulation. Symbols are as in Fig. 8. Data from the SSP-SP, LD, and IC muscles were pooled by site (Table 2) and were for surface swimming unless otherwise indicated. Abbreviations for each snake are as in Table 1. Note the earlier onset of activity for the more posterior sites within both NF39 and EO19 and for submerged vs. surface swimming of NF34.

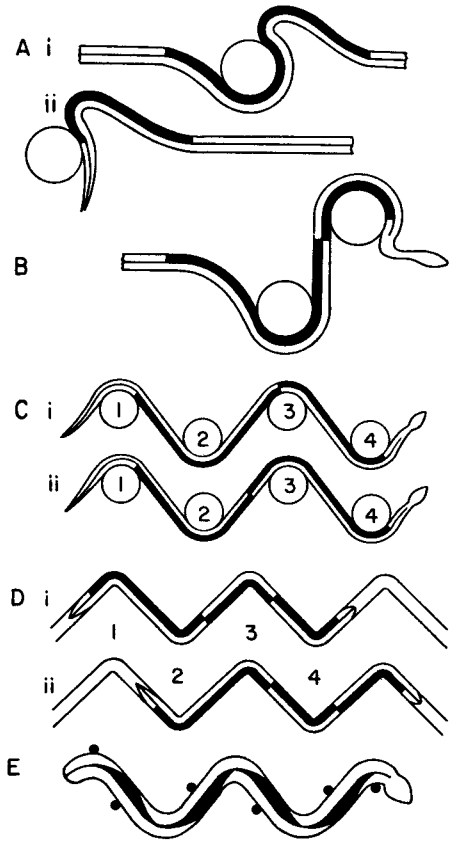


Fig. 17. Previous models predicting mechanisms of lateral undulation. All diagrams are oriented so that the snake is moving from left to right. Shaded areas indicate hypothesized regions of muscle activity. A–D are all modified from Gray and Lissmann ('50). **A:** Movement past a single peg at two points in time (i,ii). **B:** Movement past two pegs. **C:** Movement past four pegs at two points in time (i,ii). **D:** Movement through a channel with right angle bends at two points in time (i,ii). **E:** A swimming snake modified from Gray ('53). Dots indicate areas providing propulsive forces. (See Discussion for complete examination and evaluation of these models.)



time of maximal concavity rather than ceasing immediately after maximal flexion had been attained (Fig. 17). In part, this may result from their tendency to account for the position of an animal during a finite time interval rather than considering the dynamic, continuous nature of the movements characteristic of lateral undulation (Blight, '77). During their approach to understanding snake locomotion, an attempt was first made to account for the behavior of small portions of the body. Gray and Lissmann also assumed that the locomotor muscles spanned only one body segment. Although this assumption was unrealistic for the larger epaxial muscles, many of the deeper muscles do span only a few vertebrae. Yet in this study, even the activity of short muscles such as Mm. interarticularis superior and multifidus still correlated with convex-to-concave movements not predicted by Gray and Lissmann's models.

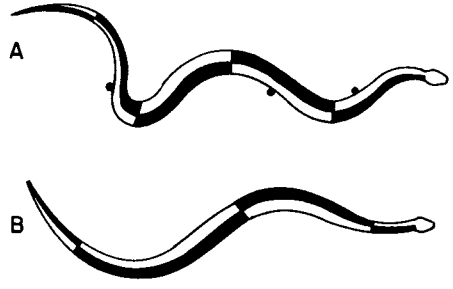


Fig. 18. Working models of the muscle activity during the lateral undulation of snakes. Shaded regions indicate active muscle. Note, because activity is traveling posteriorly, the onset and offset of activity are indicated by the posterior and anterior boundaries of each shaded area, respectively. **A:** Terrestrial lateral undulation past pegs (indicated by dots). **B:** Aquatic lateral undulation.

Not all of the aspects of the modeling of Gray and Lissmann were fully articulated. Of the assumptions that were stated, the posture of the snake on the substrate with pegs appears to have been the most problematic.

### *Swimming*

The present electromyographic records confirm that snakes swim by using alternating, posteriorly propagated unilateral muscle contractions. Figure 18B illustrates a working model of the muscle activity of swimming of snakes. The movement records indicate that a wave of lateral flexion is propagated posteriorly along the snake. However, during swimming, the relationship of EMGs to the mechanical events within the body is not constant (Figs. 16, 18B). Instead, the EMGs are propagated posteriorly faster than the mechanical wave. Therefore, there is a fundamental difference between the muscle activity during aquatic and terrestrial lateral undulation (Figs. 8, 16, 18), and Gray's ('53) emphasis of the similarities between these two modes is not supported.

Much literature is available on the hydrodynamic theory of undulatory swimming

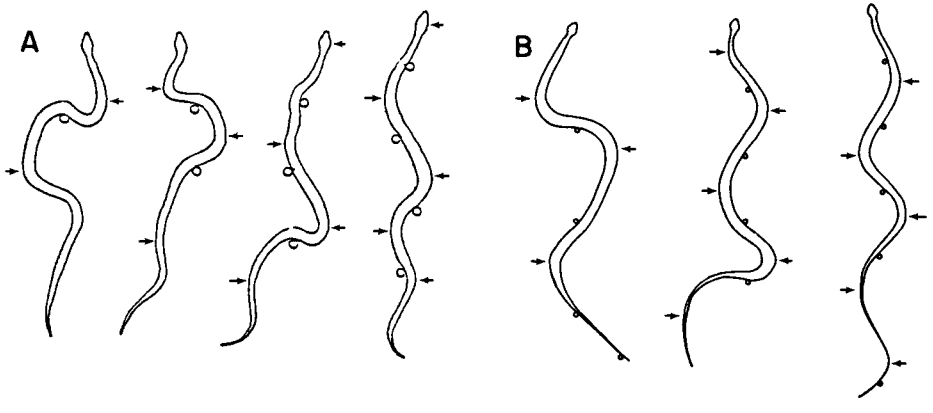


Fig. 19. Representative postures of snakes moving past a limited number of pegs. **A:** Four illustrations are tracings of films modified from Fig. 7 of Gray and Lissmann ('50). **B:** Three tracings of films of *Nerodia* from this study. The circles represent pegs and the arrows indicate approximate regions of maximum lateral displacement.

(see Webb, '75, for an extensive review). Most of this work has dealt with the locomotion of fishes, but the waveform of swimming snakes is similar to that of fish performing anguilliform swimming (Gray, '68; Hertel, '66). Much of this theoretically oriented work has predicted that an optimally efficient waveform for elongate swimmers would have regions of left and right flexion and an amplitude of undulations that increases from head to tail (Lighthill, '60); hence, the similarity of hydrodynamic constraints has been stressed for various elongate-bodied swimmers. Because eels and snakes are both such swimmers, comparison of their muscular mechanisms of swimming is useful.

Grillner and Kashin ('76) used electromyography and cinematography to study the mechanism of eel swimming. Because they were most interested in the intersegmental coordination of swimming, they implanted electrodes at four longitudinal sites to determine the propagation of EMG and mechanical waves. They found that for all points along the eel, the phase lag of the EMGs was less than that of the mechanical event within the body of the eel. Both the phase lag and duration of the EMGs decreased with increased forward velocity of the eel. Anteriorly, the muscles were active during the transition from maximal flexion on one side to maximal flexion on the opposite side. Unfortunately, it is not clear from Grillner and Kashin ('76) whether muscle activity occurred in concave or convex regions. The durations of the EMGs in the eel were usually less than one-half the time between successive onsets of activity. Thus, similarities exist between the muscular mechanisms of swimming in the eel and snake.

Grillner and Kashin ('76) found that the difference in phase lag from anterior to posterior was constant both for EMG and mechanical waves. In other words, waves (EMG or mechanical) traveled posteriorly with a constant velocity even though the two waves had different velocities with respect to each other. This constant phase lag in the eel differs from snake swimming. Table 4 indicates that the EMG phase lag of posterior sites in snakes was usually less than, or equal to, that of the more anterior sites, indicating increased speed of the EMG waves as they travel posteriorly. This pattern of muscle activity may account partially for the large anterior-to-posterior increases in amplitude, wavelength, and mechanical wave velocity that have been observed for the swimming of *Nerodia* and *Elaphe* (Jayne, '85). Sample sizes of this study are admittedly small compared to those of Grillner and Kashin ('76). Furthermore, an exception to increased EMG velocity occurred for the submerged swimming of a *Nerodia*. Presumably the eels performed submerged swimming, whereas the snakes usually swam at the water's surface. Therefore, these different phase relations between eels and snakes may indicate a difference between surface and submerged swimming rather than a difference caused by the contrasting morphologies of eels and snakes.

Blight ('77) emphasized the difficulty of predicting muscular mechanisms of undulatory swimming unless the active and the passive properties of the locomotor system are known. He modeled aspects of swimming based on various assumptions about the stiffness of the body of the swimmer. He considered stiffness-dominated vs. flexibility-dominated systems. One may envision a straight rod at rest in the water and a localized tension occurring on one side at the middle of the rod. Two different movements could result, depending on whether the rod was stiffness-dominated or flexibility-dominated. A stiffness-dominated rod would bend into a simple curve flexing toward the side of the applied tension; a flexibility-dominated rod also would form a curve in its central portion, flexing toward the side of the applied tension; however, there would be two points of inflection, as the ends of the rod would bend in the opposite direction of the central region. This would occur because the rod is not stiff enough to maintain the centrally generated concavity; instead the regions nearer the ends are dominated by the resistance of the water to their movement and they fold back on themselves, forming concavities facing the side opposite that where the tension was applied. The important point is that identical applied forces could move two systems differently, depending on the interaction of the resistive forces of the water with the stiffnesses of elongate bodies.

*TABLE 4. Mean phase lag times in seconds of EMGs and $\bar{\theta}$ during swimming*[1]

| Snake | Site1-2 | | Site 2-3 | | Site 3-4 | |
|---|---|---|---|---|---|---|
| | EMG | $\bar{\theta}$ | EMG | $\theta$ | EMG | $\bar{\theta}$ |
| NF34 | .078 ± .015(12) | .16 ± .028(6) | .11 ± .018(12) | .10 ± .044(5) | — | — |
| NF34 (submerged) | .098 ± .015(12) | .15 ± .040(8) | .12 ± .011(12) | .16 ± .032(8) | — | — |
| NF38 | .27 ± .040(8) | .31 ± .044(5) | — | — | — | — |
| NF39 (fast) | .13 ± .017(6) | .14 ± .025(6) | .052 ± .014(6) | .018 ± .047(5) | — | — |
| NF39 (slow) | .17 ± .035(4) | .22 ± .0092(4) | .11 ± .035(6) | .26 ± .013(4) | — | — |
| EO20 | .11 ± .029(6) | .14 ± .050(3) | .11 ± .020(6) | .14 ± .050(3) | .067 ± .023(6) | .11 ± .053(3) |
| EO19 | .14 ± .033(8) | .16 ± .066(5) | .096 ± .022(8) | .16 ± .038(6) | — | — |

[1]Values are given with ±95% confidence limits and with sample sizes in parentheses; see text for explanation.



The underlying concept of stiffness discussed by Blight has great intuitive appeal for snakes, elongate organisms with tremendous variation in their axial morphology. Blight dealt with such radically different chordates as *Branchiostoma,* and newt and lamprey larva. Despite the different numbers of vertebrae in *N. fasciata* and *E. obsoleta* (Table 1), no major differences were found in their mechanisms of swimming, as reflected by the relation of $\bar{\theta}$ to EMG. Assuming that equal lateral flexion could be attained for each vertebral joint in both species, the greater number of vertebrae in *E. obsoleta* would seem to make it more flexible than *N. fasciata*. However, given the overwhelming hydromechanical constraints that tend to unify elongate swimmers, the difference in flexibility between these two taxa may be trivial compared with those discussed by Blight.

### *Anatomical considerations*

The correlation of muscle activity to changes in lateral flexion was grossly similar for the lateral undulation of *Nerodia fasciata* and *Elaphe obsoleta*. However, because of the different relations of numbers of vertebrae and segmental lengths of muscles in these species, it is worthwhile to examine the extent of vertebral flexion ($\bar{\theta}$) and the numbers of simultaneously active segments to determine if there are more subtle differences between these two species.

Maximal $\bar{\theta}$ of *Nerodia fasciata* during terrestrial lateral undulation was usually near 5°. Interestingly, the slowest sequence of this mode for *N. fasciata* had the highest value of maximum $\bar{\theta}$. The values of $V_r$ of this slow sequence were rather variable even though the coefficient of variation was low enough to indicate the mode was lateral undulation. Perhaps there is a range of values of maximal $\bar{\theta}$ over which a constant $V_r$ is most easily maintained during terrestrial lateral undulation. Maximal $\bar{\theta}$ of the *Elaphe obsoleta* performing terrestrial lateral undulation was slightly less than that of *N. fasciata;* however, the complicating effects of peg spacing and snake size inhibit further comparisons between these taxa for this locomotor mode.

As mentioned previously (Table 3), the maximal $\bar{\theta}$ for a given region of a snake may vary through time and among different regions within the body of a particular snake. Allowing for this variation, swimming *Nerodia fasciata* still showed consistently greater values of $\bar{\theta}$ (2.8° to 5.0°) than *Elaphe obsoleta* (1.3° to 2.3°). These lower values for *Elaphe* are consistent with descriptions of the waveform for the swimming of these two genera. Jayne ('85) found that the waveforms of swimming *Nerodia fasciata* and *Elaphe guttata* were nearly identical after correcting for the speed and size of swimming snakes. This similarity was somewhat puzzling because *Elaphe* has about twice as many body vertebrae as *Nerodia;* therefore, one might expect *Elaphe* (with similar or shorter segmental lengths of major epaxial muscles) to have a greater number of undulations than *Nerodia*. Because *Elaphe* has similar amplitudes and wavelengths for its undulations, compared to *Nerodia, Elaphe* has nearly twice as many vertebrae in each half-wave of its body. Thus, the values of $\bar{\theta}$ of *Elaphe,* which were about half those of *Nerodia,* agree very closely with the observed waveform of these swimming snakes.

Simple differences in the number of vertebrae and their angular displacements are one of the easier aspects of axial morphology and function to deal with, yet, the concomitant variation in packaging of the axial muscles is also a topic of central interest to the study of snake locomotion. Segmental length of axial muscles is not just correlated with number of vertebrae: these two characters also correlate with specialization for habitat and habits (Gasc, '74; Jayne, '82). The proliferation of serially homologous axial elements within snakes raises some interesting issues. For example, what is a functional unit in these many-segmented,

elongate organisms? One may consider individual serial homologs as the fundamental functional units. In another sense, an entire region of the body may also be considered a functional unit because it may be spanned by a single muscle segment. If there is a fundamental unit of nervous control, this may also define a functional unit. For example, a nerve impulse could be propagated along the animal, causing the simultaneous activity of several body segments such that the number of involved segments should be considered a functional unit.

Relevant to these issues is the number of adjacent muscle segments that are simultaneously active during snake locomotion. For lateral undulation, there appear to be continuous waves of descending stimuli. Electrodes could not be put into all the simultaneously active adjacent muscle segments, but the number of such adjacent segments can be determined indirectly. If overlap in activity is observed for homologous muscles along the same side of the body at locations that are less than 180° out of phase, then one can deduce that all the intervening segments are also active. Approximate number of active adjacent segments will equal (duration of EMG) × (number of vertebrae between sites)/(lag time of EMG between two sites).

The most information of this sort is available from the swimming of *Nerodia* and *Elaphe*. The SSP-SP, LD, and IC were simultaneously active at the same level of the body during swimming; therefore, when serially homologous muscles were not available between two sites, any one of these three muscles was used for the estimate.

The phase lags (Table 4) and consequent estimates of active segments (Table 5) of *Nerodia* 34 appear somewhat anomalous. As discussed earlier, submerged swimming may account for some of these differences. Another confounding factor may be that this was the relatively stoutest *Nerodia* for which swimming was studied (comparing total length to midsagittal area in Table 2). A recent discussion has indicated that shape affects efficiency of swimming in snakes (Graham et al., '87), and it seems likely that shape could also affect the muscular mechanism of swimming.

Table 5 summarizes the estimated numbers of active adjacent segments for the swimming of *Nerodia* and *Elaphe*. Blocks of active muscle ranged from 30 to 83 in *Nerodia* and from 47 to 101 segments in *Elaphe*. Except for *Nerodia* 34, the number of active adjacent segments usually increased from anterior to posterior (Table 5).

*TABLE 5. Estimates of numbers of simultaneously active adjacent muscle segments during swimming*

| Snake | Site 1-2 | Site 2-3 | Site 3-4 |
|---|---|---|---|
| NF34 | 58 | 41 | — |
| NF34 (submerged) | 56 | 54 | — |
| NF38 | 30 | — | — |
| NF39 (fast) | 31 | 83 | — |
| NF39 (slow) | 42 | 54 | — |
| EO20 | 58 | 47 | 90 |
| EO19 | 69 | 101 | — |

Thus, a difference in the swimming of *Nerodia* vs. *Elaphe* finally seems to emerge: namely, more adjacent muscle segments are active simultaneously in *Elaphe* compared to *Nerodia*. Paired comparisons can be made between *Elaphe* and *Nerodia* for regions of the snakes that occupy similar proportional positions, as measured by either vertebral counts or distance along the body (Table 2). For the surface swimming of *Nerodia*, average sizes of blocks of active muscle segments in anterior and posterior regions were 40 and 59, respectively. In *Elaphe* these quantities were 63 anteriorly and 74–90 posteriorly. Hence, the observed similarity of waveform between these two taxa occurs by *Elaphe* simultaneously using more vertebrae, less lateral flexion per joint, and more active muscle segments for each wave, compared with *Nerodia*.

The posterior increase in numbers of active adjacent segments, correlated with the waveform of swimming snakes, suggests yet another difference between aquatic and terrestrial undulation. During terrestrial lateral undulation, there is a relatively constant configuration of the body of a snake as it passes a particular pivotal point. Furthermore, there is a fairly constant relation of the EMG to the flexion in the snake's body as it passes such a point (Fig. 7). Therefore, during terrestrial lateral undulation, a constant-size block of muscle activity may be propagated posteriorly, whereas the number of segments in such a block of active segments increases posteriorly in swimming snakes.

Thus, it appears that for both types of lateral undulation of snakes, large blocks of the major epaxial muscle segments are propagated posteriorly in a descending, unilateral fashion. Frequently such blocks of muscle activity may exceed a third of the snake's body length, and there are interspecific differences in the size of such blocks during swimming. The correspondence between a block of activity and the configuration of the body to the substrate during terrestrial lateral undulation contrasts with the situation in swimming. Consequently, some interesting questions arise about the necessary feedback mechanisms and the fineness of control snakes may have for their movements during lateral undulation on different substrates. For example, is less feedback required for swimming than for moving on irregular terrestrial substrates? Does fineness of control decrease as segmental length of muscles increases? Finally, it is known that within snakes a single muscle segment may be innervated either by one nerve from a single body segment or by many branches of nerves from several body segments (Gasc, '81), and this may be another morphological indicator of interesting interspecific differences in locomotor control and versatility.



ACKNOWLEDGMENTS

This work was completed as part of a Ph.D. dissertation submitted to the Department of Zoology at Michigan State University. Financial support was provided by National Science Foundation Dissertation Improvement Grant No. BSR-8401874 and grants from Michigan State University and National Chapters of Sigma Xi, The Research Society, as well as from NIH grant NS16270 to J. Edwards. J. Edwards, my advisor, provided much encouragement and support throughout my dissertation work, and he and G. Lauder offered many insightful criticisms of an earlier draft of this manuscript. D. Straney and J. Vorro provided necessary facilities and equipment. P. Ocello, C. D'Haem, C. Cheng, K. McWilliams, S. DosReis, J. Zablotny, C. Griffith, and C. Jayne helped with animal care and filming. J. Zablotny prepared the muscle illustrations.

LITERATURE CITED

Blight, A.R. (1977) The muscular control of vertebrate swimming movements. Biol. Rev. *52*:181–218.

Edwards, J.L. (1985) Terrestrial locomotion without appendages. In M. Hildebrand, D.M. Bramble, K.F. Liem, and D.B. Wake (eds): Functional Vertebrate Morphology. Cambridge: Belknap Press of Harvard University Press, pp. 159–172.

Gans, C. (1974) Biomechanics. An Approach to Vertebrate Biology. Ann Arbor: University of Michigan Press.

Gans, C. (1984) Slide-pushing—a transitional locomotor method of elongate squamates. In M.W.J. Ferguson (ed): Symp. Zool. Soc. London No. 52. London: Academic Press, pp. 13–26.

Gans, C. (1985) Limbless locomotion—a current overview. In Proceedings International Symposium on Vertebrate Morphology. Stuttgart and New York: Gustav Fischer Verlag, pp. 13–22.

Gasc, J.P. (1967) Introduction a l'étude de la musculature axiale des squamates serpentiformes. Mem. Mus. Natl. Hist. Nat., Ser. A Zool. *48*:69–124.

Gasc, J.P. (1974) L'interprétation fonctionelle de l'appareil musculosquelettique de l'axe vertébral chez serpents (Reptilia). Mem. Mus. Natl. Hist. Nat. Ser. A Zool. *83*:1–182.

Gasc, J.P. (1981) Axial musculature. In C. Gans and T.S. Parsons (eds): Biology of the Reptilia, Vol. 11. New York: Academic Press, pp. 355–435.

Graham, J.B., W.R. Lowell, I. Rubinoff, and J. Motta (1987) Surface and subsurface swimming of the sea snake *Pelamis platurus*. J. Exp. Biol. *127*:27–44.

Gray, J. (1946) The mechanism of locomotion in snakes. J. Exp. Biol. *23*:101–120.

Gray, J. (1953) Undulatory propulsion. Quart. J. Micro. Sci. *94*:551–578.

Gray, J. (1968) Animal Locomotion. London: Weidenfield and Nicholson.

Gray, J., and H.W. Lissmann (1950) The kinetics of locomotion of the grass snake. J. Exp. Biol. *26*:354–367.

Grillner, S., and S. Kashin (1976) On the generation and performance of swimming in fish. In R.M. Herman, S. Grillner, P.S.G. Stein, and D.G. Stuart (eds): Neural Control of Locomotion. New York: Plenum Press, pp. 181–201.

Hertel, H. (1966) Structure, Form and Movement. New York: Rheinold.

Jayne, B.C. (1982) Comparative morphology of the semispinalis-spinalis muscle of snakes and correlations with locomotion and constriction. J. Morph. *172*:83–96.

Jayne, B.C. (1985) Swimming in constricting (*Elaphe g. guttata*) and nonconstricting (*Nerodia fasciata pictiventris*) colubrid snakes. Copeia *1981*:195–208.

Jayne, B.C. (1986) Kinematics of terrestrial snake locomotion. Copeia *1986*:915–927.

Lighthill, M.J. (1960) Note on the swimming of slender fish. J. Fluid Mech. *9*:305–317.

Mosauer, W. (1932) On the locomotion of snakes. Science *76*:583–585.

Mosauer, W. (1935) The myology of the trunk region of snakes and its significance for ophidian taxonomy and phylogeny. Publ. Univ. Calif. Los Angeles Biol. Sci. *1*:81–121.

Webb, P.W. (1975) Hydrodynamics and Energetics of Fish Propulsion. Bull. Fish. Res. Bd. Canada (190).